Static Analysis On Wing Spar Joint For An Aircraft Using Finite Element Method

[1]Pavan G, [2]Manjunath M V

Assistant Professor, Don Bosco Institute Of Technology, Bangalore

_____

Abstract - **Aircraft is a highly complex flying structure which undergoes various stresses during operation. Generally transport aircraft undergoes nominal manoeuvring flights. During take-off and landing, wing produces maximum lift and it undergoes highest bending moment. The bending moment will be maximum at the root of the wing. The bending moment and shear loads from the wing are transferred to the fuselage through the attachment joints. This paper deals with stress analysis of wing spar joint. The stress analysis was carried out for wing-spar joint using Finite Element Method (FEM). Prediction of the fatigue life of wing-spar joint in a transport aircraft was precisely made. The proposed aircraft structure uses materials such as Heat Treated AISI-4340 for T section joint and Aluminum Alloy– 2024-T351 for I-section wing spar and rivet joints. Fatigue life calculation was carried out for typical service loading condition using constant amplitude S-N data for various stress ratios and local stress at various stress concentration. In this work estimation of fatigue life for crack initiation of spar joint structure were carried out at maximum stress location.**

Keywords **- Finite element approach, stress analysis, C clamp joint structure, static analysis, fatigue analysis.**
_____

1. INTRODUCTION

Now a days the stress analysis and fatigue life[1] prediction for spar joint in an aircraft wing using finite element method. The use of finite element method (FEM) for the estimation of fatigue life has been proved as a good alternative to the experimental method [1]. The main function of the wings in aircraft is to provide lift. The wings have been classified as two essential parts, the internal wing structure consists of spars, ribs, stringers, and the external wing structure consists of skin. Spar is a heavy beam in which different transverse shear load and shear bending is acting on the spar beam. It usually consists of thin panel (web) with a cap or flange at the top and bottom. Ribs are also used in the span wise distribution. The work undertaken at present incorporates the outline and investigation of the flight part utilizing the variable loads located on the spar. Normally, in aircraft the outline is done by dividing the spars into two sections. The investigation is done by utilizing the FEM packages MSC NASTRAN and MSC PATRAN. AL2024-T351 material is used in this analysis. It is found that the maximum stress is induced are within allowable limits. Additionally in the basic part the fatigue failure is generated due to high tensile stress acting on the critical region, a necessary fatigue calculation is carried out on the maximum stress. The fatigue damage value is found within the critical damage, thus assuring the validity of a design.
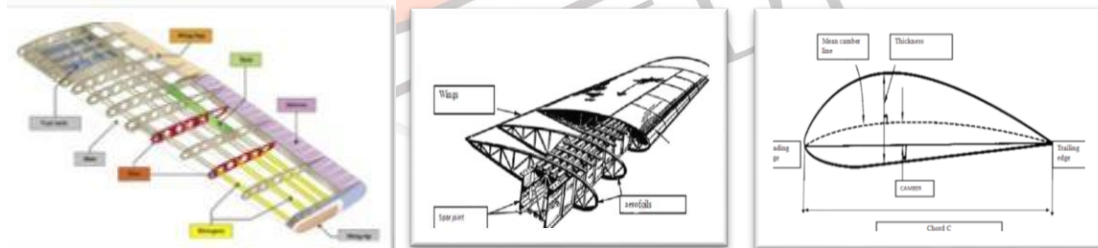
Schematic diagram of two wing spar joint

2. METHODOLOGY

In this study the wing spar joint is considered for a detailed analysis. The C section joint is considered as a multi row riveted joint under the action of tensile in plane load due to wing bending. Stress analysis of the joint is carried out to compute the stresses at rivet holes due to by-pass load and bearing load. The objective of the present work is to design and analysis of wing spar joint for a Transport Aircraft Structure to compute the stresses at rivet holes due to tension with the help of MSC PATRAN and MSC NASTRAN. The flow chart is shown in bellow figure

_____
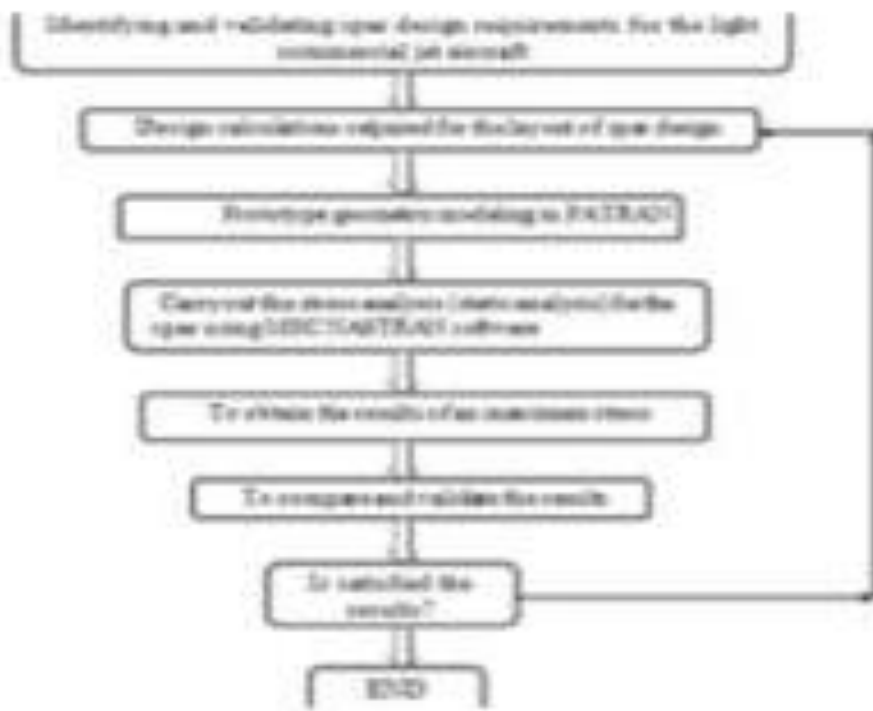
Flow chart of a static load analysis

3. GEOMETRICAL CONFIGARATION

The spar is modeled in CATIA as shown in bellow figure. It consists of different structures. , spar is considered as one of the major component in the wing. Usually spar is used as a lifting capacity of the aircraft. Majority of the weight is acting on the spar usually spar is attached to the ring and one end of the spar is connected to the fuselage and other end is act as a free edge, so an obtained spar is a cantilever beam. Each part is modeled in CATIA software. The wing spar joint with finite element properties is shown in bellow figure.
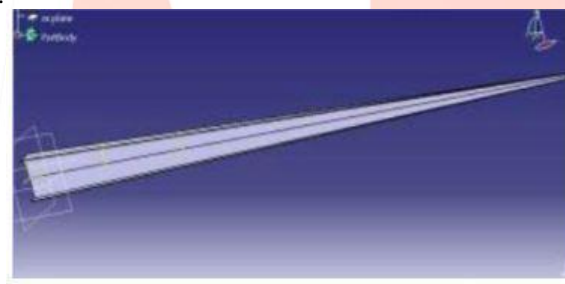
Design of uniform spar

The spar is modeled in CATIA as shown in Fig.6. It consists of different structures. , spar is considered as one of the major component in the wing. Usually spar is used as a lifting capacity of the aircraft. Majority of the weight is acting on the spar usually spar is attached to the ring and one end of the spar is connected to the fuselage and other end is act as a free edge, so an obtained spar is a cantilever beam. Each part is modeled in CATIA software. The wing spar joint with finite element properties is shown in bellow figure.
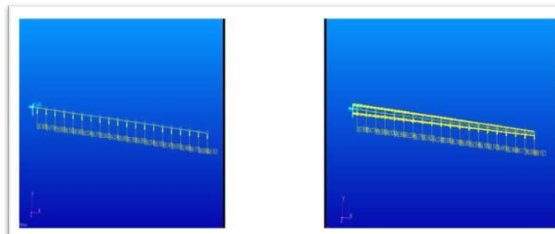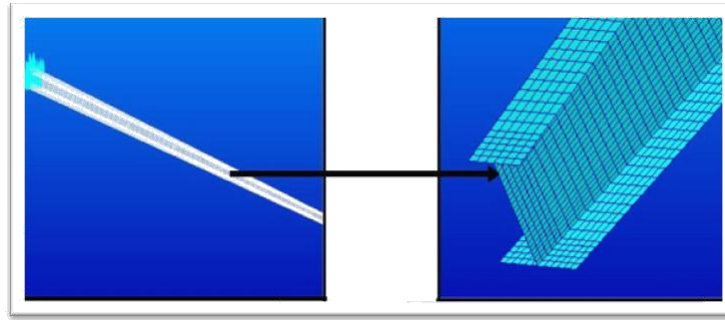

Geometric models for 1D analysis

Finite element model of spar joint

3.1. Chemical Composition

The Al 2024-T351 is used in current spar joint due to high strength and fatigue resistance properties. The chemical composition of Aluminium (Al) alloy and the physical properties of Al alloy are shown in Table.1 and Table.2.

Table 1 Chemical composition of Al alloy

COMPONENT	Wt. %
Al	90.7-94.7
Cr	Max 0.1
Cu	3.8-4.9
Fe	Max 0.5
Mg	1.2-1.8
Mn	0.3-0.9
Other, each	Max 0.05
Other, total	Max 0.15
Si	Max 0.5
Ti	Max 0.15

Table 2 Physical properties of Al alloy

Young's Modulus	7000 kg/mm^2
Poisson's Ratio	0.3
Density	2800 kg/mm^3
Yield strength	28 kg/mm^2
Ultimate strength	47kg/mm^2

4. LOADS ON THE WING BOX

Uniformly varying load was applied at tip side of the spar joint and other end is fixed which is called the root side of the spar joint. A two dimensional linear static stress analysis is carried out using finite element analysis software PATRAN and MSC NASTRAN. Mesh independent stress magnitudes are obtained through iterative mesh refinement process. Aluminum 2024-T351 alloy properties are given to the Pre-processor material properties. Load corresponding to the maximum lift load on the spar is considered. The different variable loads at each section are shown in figure 4.2. Along with dimensions used for variable load at each section along with different length are shown in table 3

4.1. Load Calculation for Spar joint
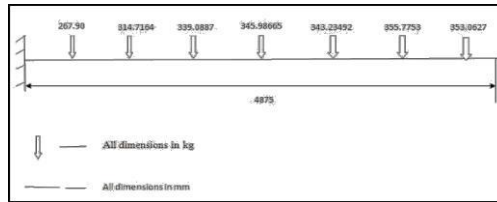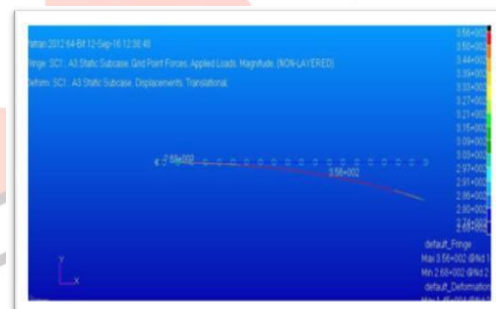

Span wise load distributions

Table 3 Span length and load distribution of spar joint

Stations	Distance from root (mm)	Loads on each section (kg)
0	0	0
1	125	267.98
2	375	314.7164
3	625	339.0887
4	875	340.9382
5	1125	345.98665
6	1375	344.23492
7	1625	345.7753
8	1875	354.0627
9	2125	354.23405
10	2375	355.0903
11	2625	355.69995
12	2875	356.089715
13	3125	356.2548
14	3375	356.16575
15	3625	355.7479
16	3875	354.8163
17	4125	352.9668
18	4375	349.1719
19	4625	340.0066
20	4875	168.1432531

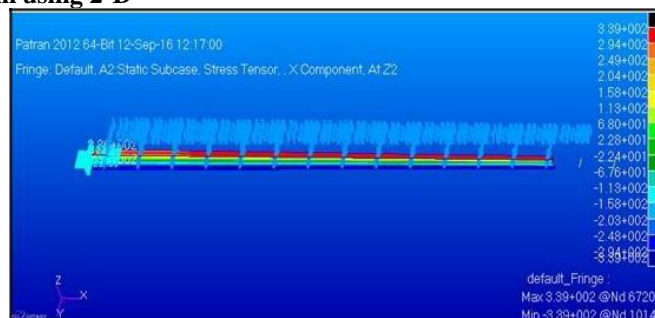### 4.2 Static analysis of spar beam using 1-D

**Static analyses of spar joint by using 1D in N/mm^2**   **Deformation of spar joint by using1D analysis.**

The static analysis is carried out by using analysis software (MSC software). The maximum stress is found to be 356 N/mm^2. However, the tensile yield strength of the aluminum 2024-T351 is 362 MPa. The induced stress level is found to be less than the allowable stress limit of the material used in the design of spar joint by using 1-D analysis. Hence, the static analysis of spar joint is considered to be safe design. Table 4.2 details the result summary of the static analysis of the spar joint using 1-D analysis.

4.3 Static analysis of spar beam using 2-D

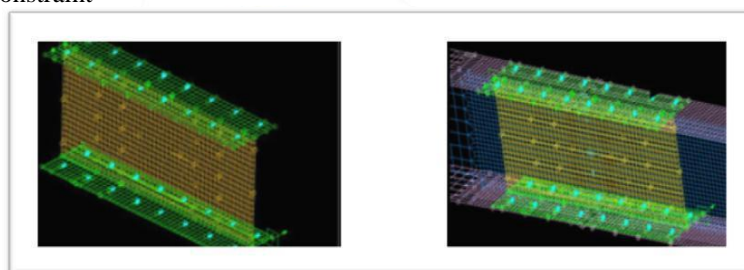Static analysis of spar beam using 2-D
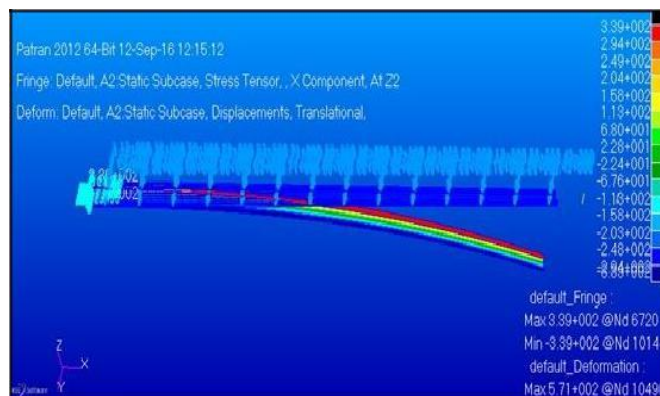
Deformation of spar beam by using 2D analysis

The maximum stress is found to be 339 N/mm². However, the tensile yield strength of the aluminium 2024-T351 is 362 MPa. The induced stress level is found to be less than the allowable stress limit of the material used in the design of spar joint by using 2-D analysis. Hence, the static analysis of spar joint is considered to be safe design. Table 4.3 details the result summary of the static analysis of the spar joint using 2-D analysis.

4.4. Local Analysis Results

As in the case of global analysis, the particular area considered for local analysis undergoes tension in bottom skin. In order to create the same surrounding, we constrain any one or two translation direction, hence we took two cases.
Case 1: With z translation constraint

Case 2: With x and z translation constraint

The directions are given to the rivets

The maximum stress is found at the one end of the rivet location, near to the bottom flange the obtained value is 327 N/mm². However, the tensile yield strength of the aluminium 2024-T351 is 362 MPa. The induced stress level is found to be less than the allowable stress limit of the material used in the design of spar joint by using 2-D analysis. Hence, the static analysis of spar joint is considered to be safe design.
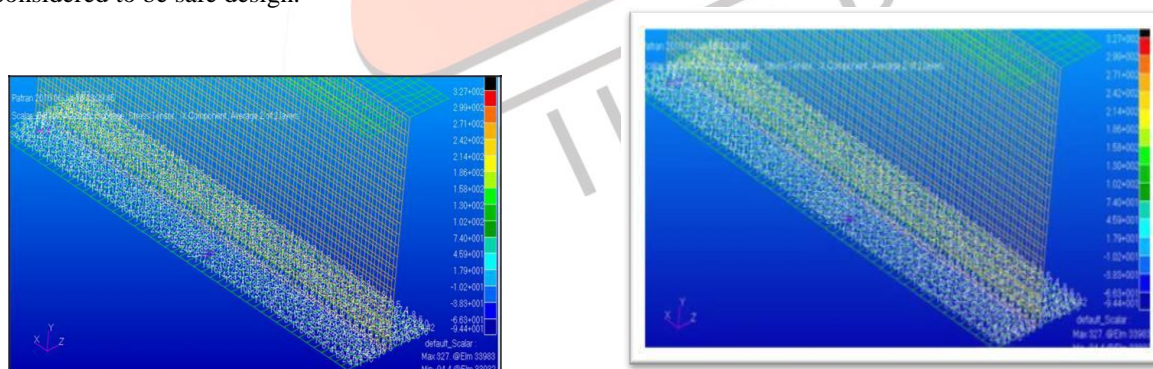
Static analysis of spar joint using 2-D   Maximum stress is obtained at 1 end of the rivet location

The maximum stress is found at the one end of the rivet location, near to the bottom flange the obtained value is 327 N/mm². However, the tensile yield strength of the aluminium 2024-T351 is 362 MPa. The induced stress level is found to be less than the allowable stress limit of the material used in the design of spar joint by using 2-D analysis. Hence, the static analysis of spar joint is considered to be safe design

4.5. Summary of Results for Iteration

Table 4 Result summary of the static analysis of the spar joint using 1-D analysis.

station	Stress (N/mm^2)
0-1	356
1-2	350
2-3	344
3-4	339
4-5	333
5-6	327
6-7	321
7-8	315
8-9	309
9-10	303
10-11	297
11-12	291
12-13	286
13-14	280
14-15	274
15-20	268

Table 5 Result summary of the static analysis of the spar joint using 2-D analysis.

station	stress(N/mm^2)
0-1	339
1-2	294
2-3	249
3-4	204
4-5	158
5-6	113
6-7	68
7-8	22.8
8-9	-22.4
9-10	-67.6
10-11	-113
11-12	-158
12-13	-203
13-14	-248
14-15	-294
15-16	-339

Table 6 Element and nodes used in C clamp joint

Parts of the spar joint	Type of element	Number of elements	Number of nodes	Aspect ratio
Top flange	Quadrilateral element	576	689	5
web	Quadrilateral element	1920	2068	5
Bottom flange	Quadrilateral element	480	3729	5
rivet	Bar	64	22	5

5. THEORETICAL CALCULATION

It is the vital step towards the design of the aircraft wing, Calculating SFD and BMD is one of the bases of analyzing beams and cantilever. Because of shear force diagram and bending moment diagram helps in design of every parameter namely spar etc. figure 4.1 shows the span wise load distribution the table 4.1 shows the span length and load distribution which helps in determining the maximum bending stress.

Table 6 Span length and load distribution of spar joint

Stations	Distance from root (mm)	Loads on each section (kg)
0	0	0
1	125	267.98
2	375	314.7164
3	625	339.0887
4	875	340.9382
5	1125	345.98665
6	1375	344.23492
7	1625	345.7753
8	1875	354.0627
9	2125	354.23405
10	2375	355.0903
11	2625	355.69995
12	2875	356.089715
13	3125	356.2548
14	3375	356.16575
15	3625	355.7479
16	3875	354.8163
17	4125	352.9668
18	4375	349.1719
19	4625	340.0066
20	4875	308.1522731

The following cantilever beam also indicates the different bending moment at different cross sections also the I sections values are tabulated in table 7. The bending stress values for each stations is calculated bellow

$$\sigma_b = \frac{\text{Bending moment}}{BD^3 - bd^3/12} * \text{max} \quad \dots\dots\dots\dots\dots\dots\dots\dots\dots\dots\dots\dots\dots\dots\dots(4.1)$$

Table 7 I section tabulated values for the spar section

Station	Bending moment (N-m)	t_w (mm)	t_f (mm)	B(mm)	D(mm)	b(mm)	d(mm)
0	17354867.98	6.65	5.9317	64.16	114.338	57.51	102.474
1	15852625.65	6.225	5.545	64.256	112.713	57.031	101.621
2	14280095.12	5.90682	5.26185	61.4382	109.463	55.526	98.9393
3	12752468.06	5.58085	4.972	59.60885	106.213	54.028	96.269
4	11296480.01	5.2365	4.6653	57.7848	102.963	52.5483	94.6324
5	9921566.846	4.8789	4.3461	55.6909	99.713	51.182	91.1208
6	8631980.708	4.5089	4.0165	54.1369	99.463	49.628	88.430
7	7429921.302	4.1284	4.678	52.313	94.213	48.1846	85.85
8	6316625.052	4.7406	4.3323	50.489	89.963	46.7486	84.29
9	5292867.121	4.3464	2.9814	48.665	86.713	45.3186	80.75
10	4359154.753	2.9491	2.65716	46.84110	84.463	44.892	78.20
11	3515815.29	2.5505	2.2724	45.017	80.213	42.4665	75.66
12	2763067.934	2.1551	1.9205	44.193	76.963	41.1379	74.72
13	2101075.371	1.76726	1.5745	41.36925	74.713	39.60194	70.56
14	1522940.509	1.53603	1.369	37.7212	67.213	37.7212	67.21
15	1050992.494	1.3267	0.85705	37.3564	66.563	37.3564	66.56
16	661757.5125	0.71424	0.63635	35.8973	64.963	35.8973	64.96
17	363436.5875	0.4304	0.384	34.073	60.713	34.073	60.71
18	1515016.15	0.1982	0.176905	32.249	57.463	32.249	57.46
19	33487.5	0.049	0.04365	30.4254	547.213	30.4254	54.21
20	0	0	0	28.6014	50.963	28.6014	50.96

From the table 4.3 we concluded that the analytical yield strength value of AL 2024 T351 material (350MPA), matches theoretical yield strength value. So the obtained design is safe. The plot of shear force, bending moment versus span length was shown bellow.
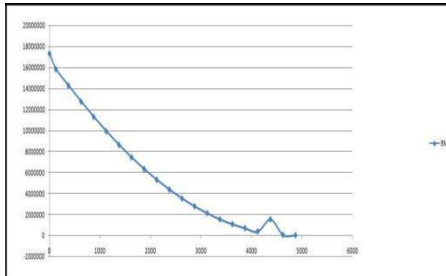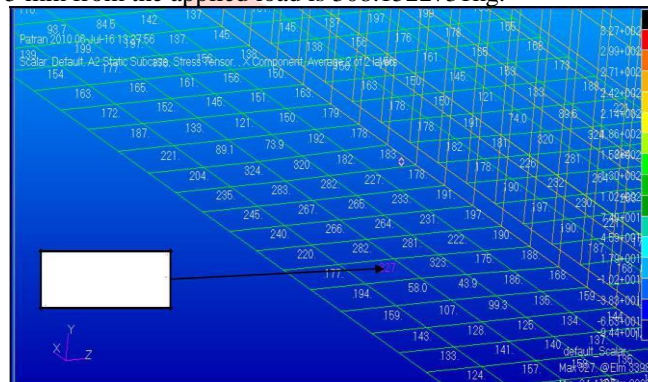

bending moment diagram of tapered
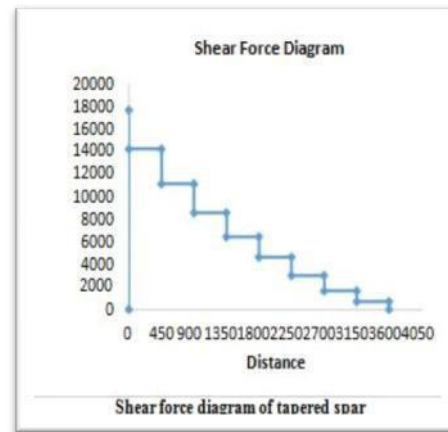
shear force diagram of tapered

6. FINITE ELEMENT ANALYSIS RESULTS

The FEM results show that the stress values which are calculated through software are given below, by taking average value of stress values at a distance of 4875 mm from the applied load is 308.1522731kg.

Maximum stress is obtained at 1 end of the rivet location

The maximum stress is found at the one end of the rivet location, near to the bottom flange the obtained value is 327 N/mm^2. However, the tensile yield strength of the aluminium 2024-T351 is 362 MPa.

7. CONCLUSION

In the present work, the finite element analysis is carried out on the wing spar joint by considering light jet aircraft structure, using MSC NASTRAN/PATRAN software. From the Static analysis, it is found that for the 1-D analysis the maximum stress obtained is 350 N/mm^2, which is well within the allowable stress of the material so an obtained design is considered to be safest design. From the Static analysis, it is found that for the 2-D analysis maximum stress obtained is 346 N/mm^2, which is well within the allowable stress of the material so an obtained design is considered to be safest design. From the Static analysis, it is found that the maximum stress obtained at one end of the rivet location is 327 N/mm^2, so the maximum stress obtained is not exactly the allowable stress of the material so obtained design is considered to be safest design.

REFERENCES

[1] Aleksandar grbovic and Bosko rasuo, "FEM based exhaustion break development forecasts for fight of lightaircraft under variable plentifulness stacking", 1st International Conference on Structural Integrity, ICONS-2014

[2] Nagarjun C M, Nagaraj V C, Byrareddy and K E Girish, "Stress Examination of Flat Tail Joint of a Vehicle Air ship and Fatigue Life Estimation", IJSRD - International Journal for Scientific Research & Development| Vol. 3, Issue 04, 2015 | ISSN (online): 2321-0613

[3] [3] Rhys Jones, Daren Peng, Pu Huang, Raman R. K. Singh, "Break development from normally happening material discontinuities in operational air ship", 3rd international conference on material and component performance under variable amplitude loading, VAL 2015.

[4] R.M. Ajaj , M.I. Friswell , M. Bourchak , W. Harasani, "Range transforming utilizing the GNATSpar wing", aeronautics and astronautics, university of Southampton, S0171BJ,UK.

[5] Harish E.R.M1, Mahesha.K2, Sartaj Patel3, " stress analysis of an wing attachment bracket for an transport aircraft structure", Vol. 2, Issue 7, July 2013

[6] Raffaele Sepe, Enrico Armentani and Francesco Caputo, "static and fatigue experiments of an full scale fuselage panel and fatigue analysis", R. Sepe et alii, Frattura ed Integrità Strutturale, 35 (2015) 534-550; DOI: 10.3221/IGF-ESIS.35.59

[7]   Polagnagu James*, Kotresh Gaddikeri , Byji Varughese and M. Subba Rao, "realization of an ideal wing test structure of an idelaised wing box", 1st International Conference on Structural Integrity, ICONS-2014 Ralph l stephens , Ali fatemi , Robert r stephens , Henry o fuchs, "metal weariness in designing",

[8]   Mohamed Hamdan A1, Nithiyakalyani S2, " design and analysis of an wing and spar of the swept back

[9]   wing",   (ISSN   2250-2459,   ISO   9001:2008   Certified   Journal,   Volume 4,   Issue
        12,   December